J Mater Sci (2009) 44:2507–2512
DOI 10.1007/s10853-009-3324-z

High speed microcompression of paper coatings

S. J. Nunnari · R. R. Farnood · M. T. Kortschot

Received: 21 April 2008 / Accepted: 5 February 2009 / Published online: 13 March 2009

Abstract A novel high speed microcompression platen tester was developed in order to measure the out-of-plane compressive modulus of thin materials. The instrument is capable of subjecting a sample of thickness 20 μm or greater to a transverse compressive pulse over a time interval ranging from approximately 2 ms to several seconds, and can therefore be used to collect data under conditions representative of those in a high speed calender nip. In this study, free layers of coating formulations normally used to coat paper were prepared and tested using the microcompression platen tester described above. Tests were conducted at high speeds, with a pulse duration of 2 ms during the compressive stroke, and at 23 °C to simulate room temperature calendering conditions. The compressive modulus of the coating did not correlate strongly with the modulus of its constituent latex. Latex content, however, strongly affected coating compressive modulus. A sharp increase in the compressive modulus was observed at the coating critical pigment volume concentration (CPVC)—essentially the latex concentration at which the coating layer porosity is reduced to zero. Pigment size distribution and pigment morphology also affected the compressive modulus of coating in a manner consistent with packing theory.

S. J. Nunnari · R. R. Farnood · M. T. Kortschot (✉)
Department of Chemical Engineering and Applied Chemistry, Pulp & Paper Centre, University of Toronto, 200 College St., Toronto, ON M5S-3E5, Canada
e-mail: mark.kortschot@utoronto.ca
URL: www.chem-eng.utoronto.ca/faculty/kortschot.html

Introduction

A thin coating layer is often applied to a paper base sheet, which is then calendered, to improve the optical and surface characteristics of the paper. Coated papers exhibit significantly improved printability and are characterized by their high degree of uniformity, smoothness, and gloss. The improvement in smoothness during calendering is related to permanent deformation of both the coating layer and the underlying base sheet. In this study, the out-of-plane stress–strain properties of coating layers were characterized using a novel high-speed compression testing machine.

Paper coatings, generally applied as an aqueous suspension, consist of an inorganic pigment, a binder, and water. When dried, the coating layer may be described as a porous network of pigment particles in which adjacent particles are bound to one another by means of a binder. The porosity of the coating layer, which can range from 15% to 40% [1], largely depends on the pigment shape and size distribution (i.e., packing properties) and the binder type and concentration [2]. Pores do not bear load, and hence the out-of-plane coating stiffness of a porous coating is lower than that of a less porous or pore-free coating. Thus, the stiffness, or elastic modulus, of the coating layer in the out-of-plane direction is highly dependent on the pigment and binder type and the resulting porosity of the dry coating structure.

LePoutre and Rigdahl [1] studied the effect of porosity and pigment shape on the stiffness of coating layers. Using composite theory it was shown that the in-plane stiffness of coating layers can be predicted based on knowledge of the porosity, elastic modulus of the pigment and binder, the amount of binder, and pigment shape [1]. Prall et al. [3] also established that porosity and pigment and latex content affect the in-plane modulus of coating layers. Similarly, it was shown by Kan et al. [4] that the viscoelastic properties of paper coatings were dependent on the viscoelastic properties of the binder and pigment, their respective volume fractions, and the coating porosity. Furthermore, Kan et al. [4] also demonstrated that the coating viscoelasticity was correlated to the compressive behavior of coated paper during calendering.

Rättö [5] and Wikström et al. [6] investigated the out-of-plane compression behavior of coatings and found results similar to those produced by the studies of in-plane properties. In both studies, a cast coating layer, ∼2–3 mm thick, was compressed and the stress–strain response was measured. It was determined that the compression behavior of the coating layer was highly dependent on the porosity and latex content. However, it is possible that the unrealistically thick coating layers used are not wholly representative of 5 to 20 μm thick coating layers typical in commercial samples. In fact, Wikström et al. [6] showed that thinner layers exhibit a much higher deformation during loading than their thicker counterparts. Barbier et al. [7] developed a method to characterize relatively thin coating layers, 30 and 70 μm thick, using microindentation, allowing the out-of-plane elastic modulus to be computed. The coating microstructure was changed in this study by changing the type of pigment used, but the viscoelastic properties of the coating, and the effect of strain rate on coating behavior were not measured.

In this work, the compression behavior and out-of-plane stiffness of very thin free coating layers at high strain rates were investigated. The effect of varying the latex type, latex content, and particle shape and size distribution on compression behavior was also explored.

Equipment

A novel high speed microcompression platen tester was developed for this study in order characterize the out-of-plane compressive behavior of thin free coating layers (>20 μm). Using a high-resolution linear actuator, a maximum displacement of 60 μm and a compressive force of up to 1 kN can be achieved. A load cell measures the compressive force generated as the actuator expands and compresses a sample between two circular compression platens with a diameter of approximately 0.86 mm. The degree of misalignment between the two compression platens is roughly 5 μm end-to-end. Both the actuator and load cell are connected to an analog/digital converter allowing for continuous, real-time acquisition of displacement and force data.

Parameters, such as the maximum displacement, pulse duration, and pulse shape (for example: ramp, triangle, sine, etc.) are defined prior to performing a compression test using the control software. Generally, a maximum actuator displacement corresponding to 20 percent compressive strain (approximately 10 μm) and a simple ramp pulse were used. A ramp displacement pulse was used as it allowed for sample loading at a constant rate. The pulse duration may also be varied from approximately 2 ms to 4 s during the compressive stroke depending on the type of test. All tests were conducted under TAPPI T402 om-88 standard controlled humidity and temperature conditions: 23 °C + 1°, 50% RH ± 2%.

Materials and methods

One commercial ground calcium carbonate pigment, HYDROCARB® 90 (OMYA, Perth, Ontario, Canada), and three experimental kaolin clay pigments (IMERYS, Sandersville, Georgia, USA) with varying particle size distributions and shape factors were used in this study. Four commercial styrene–butadiene latexes were also used in this study (Styronal® NX 4222 X, Styronal® NX 4515 X, Styronal® BN 4606 X, Styronal® ND 656) (BASF Canada, Mississauga, Ontario, Canada). Relevant pigment properties are listed in Table 1. It should be noted that narrowness is defined as:

$$\frac{D_{30}}{D_{70}} \times 100\%$$

where D_{30} and D_{70} are the cumulative masses of particles within a particle size distribution with diameters less than or equal to 30 and 70 μm, respectively. Shape factor is an average measurement of the aspect ratio for a population of particles with a distribution of both size and shape; effectively the weight averaged aspect ratio of the population [8].

Coating colors were prepared in a lab-scale batch technique in which each component was individually added to a beaker agitated by a lab-scale mixer. In addition to this, coatings were also degassed using an aspirator. The required dry amounts of pigment, binder, and dispersant added to a coating color were calculated based on a simple mass balance with water added as a dispersion medium. If necessary, the pH of the coating color was adjusted to

Table 1 Relevant pigment properties

Pigment	Type	Particle size		
		Median (μm)	Narrowness	Shape factor
HC90	GCC	0.700	–	–
K3	Kaolin	0.346	26.4	13
K6	Kaolin	0.452	48.0	17
K7	Kaolin	0.670	14.3	19

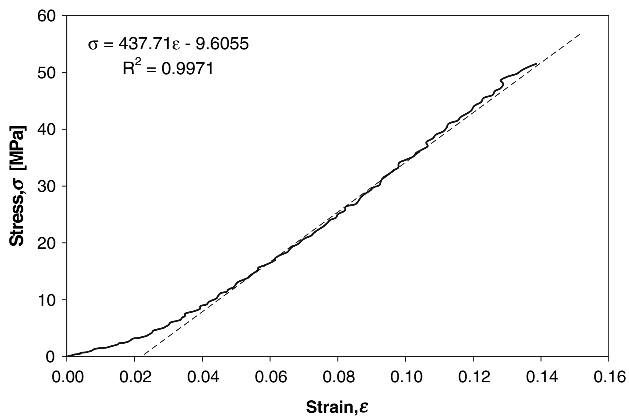

Fig. 1 A stress–strain curve obtained from compression testing of a latex film (glass transition temperature, T_g, of −25 °C) illustrating the region over which the compressive modulus is extracted

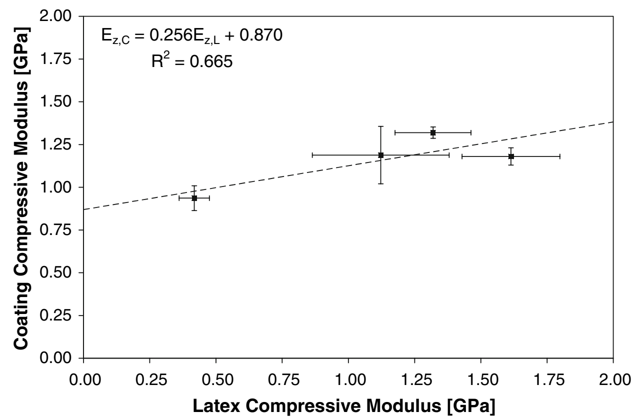

Fig. 2 Coating compressive modulus plotted as a function of the compressive modulus of its constituent latex reveals that the two moduli are only weakly correlated. Error bars represent the 95% confidence interval, $n = 5$. Coatings were prepared using a GCC pigment

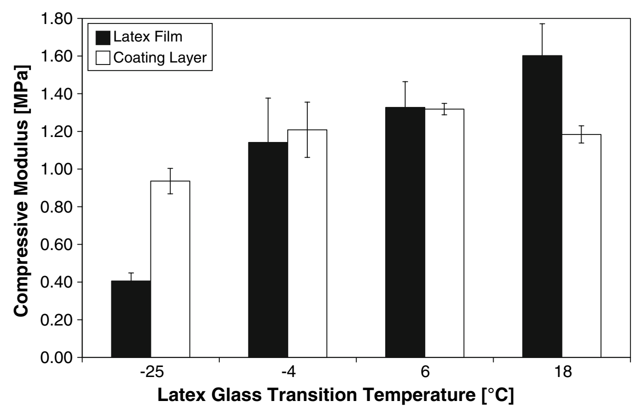

Fig. 3 Comparison of compressive modulus of latex films and free coating layers containing the same latex obtained under dynamic conditions. Error bars represent 1 standard deviation, $n = 5$. Coatings were prepared using a ground calcium carbonate pigment

between 8 and 9 with 0.5 molar sodium hydroxide. A solid content of 65 percent by weight was used throughout this study.

A polyester film substrate (LOOK Oven Roasting Film, TERINEX, England) was coated on a bench-top laboratory coater using a #24 metering rod following a method based on the work of Prall [9]. The coating was allowed to dry at 110 °C for 5 min in the drying chamber of the coater. Coated polyester samples were conditioned at 23 °C and 50% relative humidity for 24 h. The coating layer was then peeled from the polyester substrate and cut into squares, roughly 5 × 5 mm^2, for testing. Care was taken to avoid bending the sample while slowly separating the coating layer and polyester substrate.

A ramp displacement pulse was used with a pulse duration of 4 ms for the compressive stroke. A 4 ms pulse was selected, as it is comparable to the time spent by the coated paper web in the nip of a typical commercial calender. The amplitude of the displacement pulse was set to be equivalent to approximately 20% of the sample thickness. All tests were performed at 23 °C. The strain, or more specifically the compressive strain, is simply the engineering strain and the Young's modulus was obtained through linear regression of the initial linear portion of the stress–strain curve, as illustrated in Fig. 1.

Results and discussion

The effect of latex T_g

Figure 2 illustrates a positive correlation between the compressive modulus of the coating and latex, E_z, where latex modulus increases with glass transition temperature. The correlation is relatively weak, indicating that the modulus of latex may have only a minor effect on the overall modulus of the coating structure. Figure 2 also reveals that while coatings prepared with latexes of intermediate stiffness have a compressive modulus comparable to their pure latex constituent, the same is not true for coatings consisting of very hard or soft latexes. This observation is more clearly illustrated in Fig. 3. The latex films exhibited a range of moduli, but the compressive moduli of all the coatings were relatively similar.

It has been demonstrated that upon drying, stiff latexes tend to shrink less than softer latexes [10], producing a more porous or less dense structure, which, in turn, may be relatively less stiff. Such behavior could account for the lack of strong correlation between the latex and coating moduli. This was investigated further using mercury intrusion porosimetry. Figures 4 and 5 illustrate the porosity and pore size distribution of the different coatings based on their latex

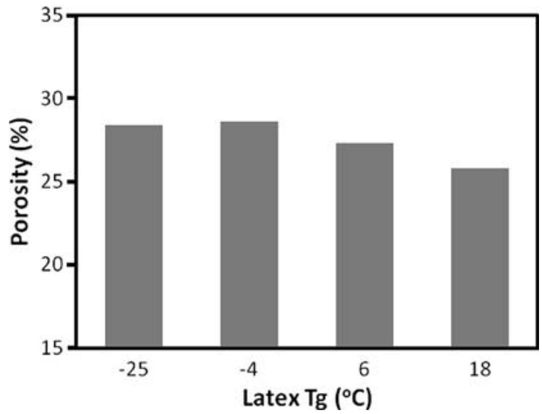

Fig. 4 Porosity measurements for free coating layers prepared using latexes with different glass transition temperatures

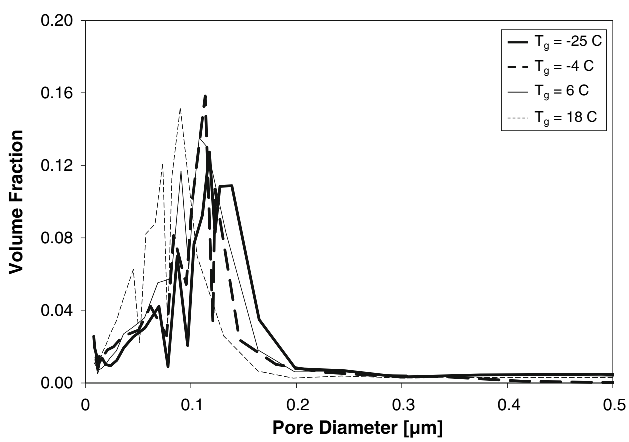

Fig. 5 Pore size distribution measurements for free coating layers prepared using latexes with different glass transition temperatures

T_g. It can be seen that while the porosities of each coating do not differ significantly, the pore size distributions indicate the presence of overall smaller pores in coatings containing latexes with higher glass transition temperatures. Thus a mechanism in which the collapse of pores affects the mechanical response of coatings under compression is perhaps more suitable than one in which the deformation of latex bridges is solely considered. A similar mechanism for the increase in gloss as a result of coating compaction has been proposed by other authors [2].

The effect of latex content

Figure 6 is a collection of SEM micrographs showing the surface and cross section of several coatings with various pigment volume concentrations (PVCs). The transition from a porous pigment-latex structure to a material which is continuous in the latex phase is clearly visible. Of particular importance are the images corresponding to PVCs of 60 and 45. Over this range the coating structure transitions from a porous network of pigment particles to a nonporous pigment reinforced polymer. As this transition occurs pigment particles become entirely surrounded by latex and the interstitial voids between adjacent particles are filled with latex. The PVC at which the porosity of the structure is effectively reduced to zero is termed the critical pigment volume concentration (CPVC). For the GCC/latex coating presented in Fig. 6, the CPVC exists within the PVC range of 60 to 45.

The CPVC for a given pigment may be identified in a number of ways, but is typically characterized by sharp transitions in such properties as porosity, gloss, brightness, and opacity [11, 12]. As shown in Fig. 7 a similar trend is observed for compressive modulus.

Over the PVC range from 90 to 60, the modulus of the coating increases as more latex is introduced into the coating structure. With the addition of latex, the mechanically weak air-filled pores present throughout the coating structure at higher PVCs are effectively replaced by regions of latex and become load bearing. The incidence and severity of pore collapse, which contributes to the reduced modulus as observed at higher PVCs, is reduced and as a result the modulus of the coating increases dramatically over this range.

Below the CPVC, however, the modulus decreases and approaches the modulus of pure latex at a PVC of 0; at which point the coating is no longer a pigment–latex composite, but latex alone. This reduction in E_z is a result of the volumetric replacement of stiff pigment particles by the softer latex matrix.

The effect of particle size and shape distribution

Both the type of latex and the latex content have been shown to affect the compressive modulus of the dry coating structure. This is a result of not only the mechanical properties of the latexes themselves, but also their effect on the coating structure. However, it is pigment properties, such as size and morphology which largely define the structure of the dry coating layer.

The compressive modulus of free coating layers was observed to increase with increases in the width of the pigment size distribution. Three free coating layers were prepared using kaolin clay pigments with a similar median particle size and shape factor, but varying size distributions (as characterized by the size distribution narrowness).

In Fig. 8, the compressive modulus is plotted as a function of pigment size distribution for the free coating layers prepared using the three different kaolin clay pigments. A distinct difference between E_z of the coatings prepared with the narrowest and broadest size distributions is apparent, but there appears to be no difference between the coatings prepared using the two kaolin clays with

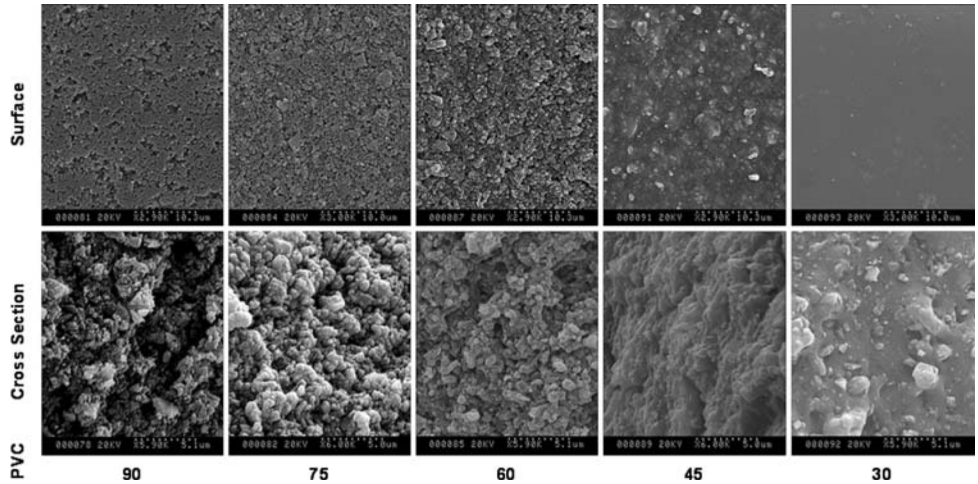

Fig. 6 SEM micrographs of free coating layers containing a GCC pigment and varying amounts of latex. A transition from a porous structure to a structure which is continuous in the binder phase occurs between a pigment volume concentration of 60 and 45. The CPVC of the coating exists in this range

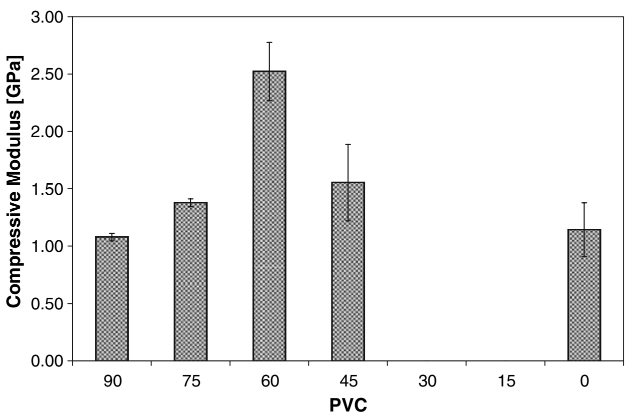

Fig. 7 The compressive modulus measured as a function of PVC under dynamic conditions. The sharp transition occurring at a PVC of approximately 60 denotes the CPVC. Error bars represent 1 standard deviation, $n = 5$

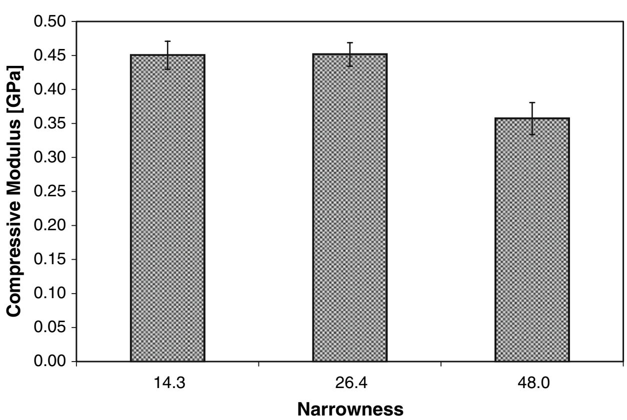

Fig. 8 Compressive modulus of coatings containing kaolins with various size distributions. Error bars represent 1 standard deviation, $n = 5$

broader distributions. This is likely due to the initially high porosity of kaolin coatings caused by the nature in which the platy kaolin particles tend to pack, the so-called 'house of cards' packing formation.

Based on packing theory it is expected that particles with a broad size distribution will form a denser structure as smaller particles may fill the interstitial space between tightly packed larger particles. Through repeated compaction of the coating layer, excessive porosity is reduced as the pigments arrange themselves into a more organized structure. Upon so doing, differences in packing efficiency based on the particle size distribution of these pigments result in structures of varying density and stiffness, as shown in Fig. 9.

The compressive modulus of free coating layers was observed to decrease with increasing aspect ratio, or shape factor. As previously described, the shape factor is an average measurement of the aspect ratio for a population of particles with a distribution of both size and shape; effectively the weight averaged aspect ratio of the population [8].

The effect of pigment morphology is most obvious when comparing the compressive behavior of coatings prepared using pigments with vastly different aspect ratios, such as a GCC and kaolin. GCC particles tend to have a low aspect ratio, essentially one, while kaolin clay pigments are platy

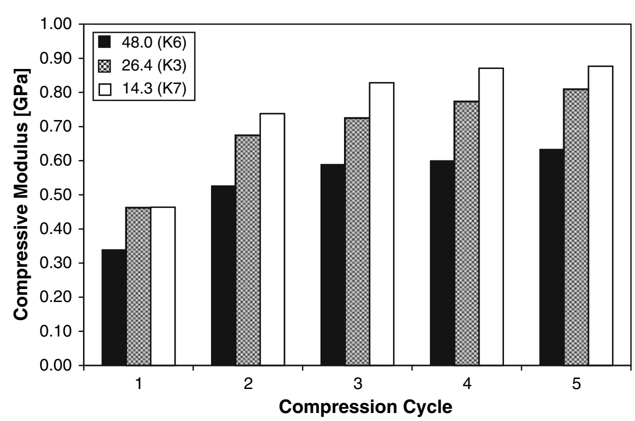

Fig. 9 Cyclical compression of coatings containing kaolin clays with various pigment size distributions (as characterized by their narrowness) reveals differences in the compressive modulus

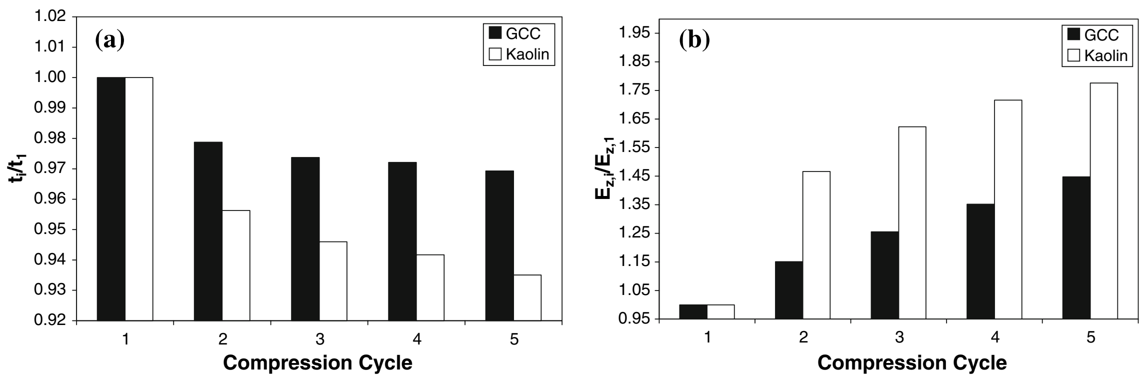

Fig. 10 **a** Reduction in thickness and **b** increase in modulus of typical ground calcium carbonate and kaolin clay coating layers with cyclic compression

in nature with large aspect ratios. Figure 10 illustrates the reduction in thickness and increase in modulus for typical GCC and kaolin coating layers. It can be seen that due to the greater initial packing efficiency of the more spherical GCC pigment particles coatings prepared using GCC tend to experience a smaller reduction in thickness and increase in modulus as a result of repeated compression.

Conclusions

The effects of latex type, latex content, and pigment shape and size distribution on coating structure and resultant out-of-plane compressive behavior was investigated in this study. It has been shown that the type of latex clearly affected the coating modulus, but latex and coating stiffness were only weakly correlated. As previously discussed, coatings prepared using different latexes had comparable compressive moduli, but some differences in overall porosity and pore size were observed. This indicates that pore collapse has a significant influence on coating compression.

Similarly, the compressive modulus of a coating depends strongly on the latex content, or pigment volume concentration. A sharp increase in the coating modulus was observed in the vicinity of the CPVC, as the coating transitions from a porous pigment–latex composite to a pigment–latex composite continuous in the latex phase.

Particle size distribution and shape factor have been shown to affect the compressive modulus of free coating layers in a manner generally consistent with simple packing theory.

Acknowledgements The authors would like to acknowledge the Surface Science III Consortium Member Companies: Hokuetsu Paper Mills, Ltd., International Paper, Oji Paper Co., Ltd., Abitibi Bowater Inc., and Tembec Industries Inc. for their financial support. We would also like to thank Mr. Roger Wygant from Imerys, and BASF Canada for providing pigment and latex samples.

References

1. LePoutre P, Rigdahl M (1989) J Mater Sci 24:2971. doi:10.1007/BF02385655
2. Larsson M, Engström G, Vidal D, Zou X (2006) Compression of coating structures during calendering. In: 2006 TAPPI advanced coating fundamentals symposium, vol 2006, p 354
3. Prall KM, Shaler SM, LePoutre PF (2000) Nordic Pulp Pap Res J 15(5):564
4. Kan CS, Kim H, Lee DI, Van Gilder RL (1997) TAPPI J 80(5):191
5. Rättö P (2004) J Pulp Pap Sci 30(12):335
6. Wikström M, Mäkelä P, Rigdahl M (2000) TAPPI J 83(8):92
7. Barbier C, Larsson P, Östlund S (2005) J Coat Technol Res 2(6):92
8. Philip J, Jones E, Pruett RJ, Yuan J, Robins W, Garska MJ, Cummings DO, Bilimoria BM, Wesley R, Assigned to Imerys Pigments Inc. (2005) Hyperplaty clays and their use in paper coatings and fillings, methods for making same, and paper products having improved brightness. US Patent 7,226,005 B2, 23 Mar 2005
9. Prall KM (1996) The viscoelastic behaviour of pigmented latex coating films. Ph.D. Thesis, Technische Universitat Graz, Austria
10. Watanabe J, LePoutre P (1982) J Appl Polym Sci 27:4207
11. Lee DI (1998) The critical pigment volume concentration concept for paper coatings: I. Model coating systems using plastic pigments and latex binders for paper coating applications. In: Proceedings of the 1998 TAPPI coating conference
12. Lehtinen E (2000) Pigment coating and surface sizing of paper. Papermaking science and technology collection, vol 11. Finnish Paper Engineer's Association and TAPPI, Helsinki